Chirped RF Pulse Generation Based on Optical Spectral Shaping and Wavelength-to-Time Mapping Using a Nonlinearly Chirped Fiber Bragg Grating

Hao Chi and Jianping Yao, *Senior Member, IEEE, Member, OSA*

***Abstract*—Chirped radio-frequency (RF) pulse generation based on optical spectral shaping and nonlinear wavelength-to-time mapping in a nonlinearly chirped fiber Bragg grating (NLCFBG) is investigated. In the proposed approach, the spectrum of a femtosecond pulse generated by a mode-locked fiber laser is shaped by an optical filter that has a sinusoidal frequency response. The spectrum-shaped optical pulse is sent to the NLCFBG, to implement nonlinear wavelength-to-time mapping. A chirped electrical pulse with the central frequency and chirp rate determined respectively by the first- and second-order dispersions of the NLCFBG is then obtained at the output of a high-speed photodetector. An approximate model that describes the chirped RF pulse generation is derived, which is verified by numerical simulations. Chirped pulse generation with a pulse compression ratio as high as 450 is demonstrated. The key device in the chirped RF pulse generation system is the NLCFBG, which is investigated in detail with an emphasis on the influence of its group delay ripples on the performance of the pulse generation system. Techniques to design and fabricate the NLCFBG are also discussed. The proposed approach provides a potential solution for the generation of chirped RF pulse with a high central frequency and large chirp rate for applications in pulse compression radar systems.**

***Index Terms*—Chirped fiber Bragg grating, chirped microwave pulse, optical signal processing, pulse compression radar.**

I. Introduction

PULSE compression is a widely used technique in modern radar systems for increasing the range resolution. Instead of transmitting sinusoidal radio-frequency (RF) pulses, in a pulse compression radar the transmitted pulses are usually frequency modulated or phase coded [1]. The pulse compression is realized at the receiver end through matched filtering. Chirped or phase-coded pulses are conventionally generated in the electrical domain using electrical circuitry. The major difficulty associated with the electrical approaches is the low central frequency and small time-bandwidth product (TBWP). On the other hand, the broad bandwidth offered by optics provides an effective solution for the generation of high-frequency and large TBWP RF pulses. An approach was recently proposed to optically generating linearly chirped RF pulses using a mode-locked fiber laser (MLFL) and two chirped fiber Bragg gratings (CFBGs) having different chirp rates [2]. The optical pulses from the MLFL were reflected from the two CFBGs to introduce different dispersions. The beating of the chirped optical pulses at a photodetector (PD) would generate a linearly chirped RF pulse. Recently, we proposed an approach to optically generating phase-coded RF pulses using an MLFL and an unbalanced Mach–Zehnder interferometer (MZI) [3], in which the phase coding was realized using an optical phase modulator that was incorporated in one arm of the MZI.

Both approaches in [2] and [3] are based on optical interference with an MZI structure. Therefore, the systems are sensitive to environmental changes, such as vibration and temperature shifts. To avoid using an MZI in a chirped RF generation system, we have recently proposed a method based on nonlinear wavelength-to-time mapping in a nonlinear dispersion media [4]. Since no optical interference is involved in the approach, the system has a better stability. In the experimental demonstration, the nonlinear dispersive element was a length of standard single-mode fiber (SSMF). Due to the limited nonlinear dispersion of the SSMF, the generated chirped RF pulses have a small TBWP. To generate chirped pulses with a large TBWP, a dispersive element with a large second-order dispersion must be used. One solution is to use a nonlinearly chirped fiber Bragg grating (NLCFBG). In this paper, we investigate the use of an NLCFBG with large first- and second-order dispersion coefficients for chirped RF pulse generation. An approximate model that describes the chirped RF pulse generation is derived, which is verified by numerical simulations. It is shown that a chirped RF pulse with a TBWP as large as 450 can be generated if an NLCFBG with a first- and second-order dispersions of 500 ps^2 and 60 ps^3 is used. In addition, a chirped fiber Bragg grating usually has group delay ripples (GDRs) even with apodization due to the errors in grating period and the refractive index modulation arising from imperfections in the fabrication process. In this paper, the influence of the GDRs on the performance of the chirped RF pulse generation is investigated in detail. The key advantage of using an NLCFBG for chirped RF pulse generation is that very high frequency RF pulses with large chirp rate can be generated using an NLCFBG.

Manuscript received August 8, 2007; revised January 9, 2008. This work was supported in part by The Natural Sciences and Engineering Research Council of Canada. The work of H. Chi was supported in part by the National Natural Science Foundation of China under Grant 60407011 and in part by the Zhejiang Provincial Natural Science Foundation of China under Grant Y104073.

H. Chi is with the Department of Information and Electronic Engineering, Zhejiang University, 310027 Hangzhou, China and also with the Microwave Photonics Research Laboratory, School of Information Technology and Engineering, University of Ottawa, Ottawa, ON K1N 6N5, Canada (e-mail: chihao@zju.edu.cn).

J. Yao is with the Microwave Photonics Research Laboratory, School of Information Technology and Engineering, University of Ottawa, Ottawa, ON K1N 6N5, Canada (e-mail: jpyao@site.uOttawa.ca).

Color versions of one or more of the figures in this paper are available online at http://ieeexplore.ieee.org.

Digital Object Identifier 10.1109/JLT.2008.917768

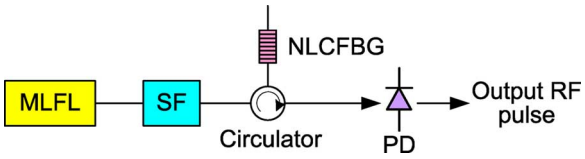

Fig. 1. Schematic diagram of the chirped RF pulse generation system based on optical spectral shaping and nonlinear wavelength-to-time mapping using an NLCFBG. (MLFL: mode-locked fiber laser; SF: sinusoidal filter: NLCFBG: nonlinearly chirped fiber grating; PD: photodetector).

II. Principle

The schematic diagram illustrating the system for chirped RF pulse generation is shown in Fig. 1. A femtosecond pulse generated from the MLFL is spectrum shaped by an optical filter that has two taps with a sinusoidal frequency response. The spectrum-shaped pulse is then sent to the NLCFBG to perform nonlinear wavelength-to-time mapping. The NLCFBG operates in the reflection mode that is connected by an optical circulator. Thanks to the nonlinear wavelength-to-time mapping in the NLCFBG, a chirped RF pulse is generated at the PD. The central frequency and the chirp rate of the generated RF pulses are determined by the values of the first- and the second-order dispersions of the NLCFBG. Therefore, by designing an NLCFBG with the desired first- and the second-order dispersions, a chirped RF pulse with the required central frequency and chirp rate can be generated. The sinusoidal filter (SF) is a two-tap optical delay-line filter, which can be a Sagnac-loop filter with a single segment of polarization-maintaining fiber in the loop [5] or an unbalanced MZI. The frequency response of the SF can be expressed as

$$H_{SF}(\omega) = \frac{1}{2}\cos\left(\frac{\omega\tau}{2}\right)\exp\left(j\frac{\omega\tau}{2}\right) \tag{1}$$

where τ is the time delay difference between the two taps.

The key component in the system for the wavelength-to-time mapping is the NLCFBG. To generate a chirped RF pulse with a large chirp rate, the NLCFBG should have a large second-order dispersion. Mathematically, the NLCFBG can be modeled as a linear time-invariant system with a transfer function given by

$$H_G(\omega) = |H_G(\omega)|\exp\left[j\Phi(\omega)\right]. \tag{2}$$

The first- and the second-order dispersion coefficients are given by $\ddot{\Phi} = \partial^2\Phi(\omega)/\partial\omega^2$ and $\dddot{\Phi} = \partial^3\Phi(\omega)/\partial\omega^3$, respectively. If the grating has only the first-order dispersion $\ddot{\Phi}$, a real-time Fourier transform can be realized given that the input pulse is confined to a small time width τ_w and the dispersion coefficient $\ddot{\Phi}$ is sufficiently large such that $\tau_w^2/|\ddot{\Phi}| \ll 1$. Therefore, the reflected signal $a_r(t)$ is a scaled version of the Fourier transform of the input signal $a_i(t)$, $a_r(t) \propto \widetilde{A}_i(t/\ddot{\Phi})$, where $\widetilde{A}_i(\cdot)$ is the Fourier transform of $a_i(t)$ [6]. In other words, a linear mapping from optical frequency to time, $\omega \rightarrow t/\ddot{\Phi}$, is implemented due to the linear relationship between the relative group delay and the frequency $t = \ddot{\Phi}\omega$. In [7], we have demonstrated a similar configuration to generate RF pulses based on wavelength-to-time mapping for radio-over-fiber applications, where a linear dispersive element was used. Thanks to the linear relationship between optical frequency and time, a sinusoidal spectrum is mapped to a sinusoidal temporal pulse with a fixed carrier frequency given by $\omega_c = \tau/|\ddot{\Phi}|$.

For an NLCFBG, however, it has both the first-order dispersion $\ddot{\Phi}$ and the second-order dispersion $\dddot{\Phi}$. According to the equation that relates the relative group delay and the dispersion parameters

$$t = \ddot{\Phi}\omega + \frac{1}{2}\dddot{\Phi}\,\omega^2 \tag{3}$$

where t is the relative group delay, the nonlinear relationship between the optical frequency and time can be expressed as $\omega \rightarrow (-\ddot{\Phi} \pm \sqrt{\ddot{\Phi}^2 + 2\,\dddot{\Phi}\,t})/\,\dddot{\Phi}$, where $\pm$ corresponds to the positive and negative $\ddot{\Phi}$, respectively. An approximate model describing the generated RF pulse, $i(t)$, which is derived based on the nonlinear relationship between the frequency and time, is given by

$$\begin{aligned} i(t) &\propto r(t)\left[1+\cos\Psi(t)\right] \\ &= r(t)\cdot\left\{1+\cos\left[\frac{\tau\sqrt{\ddot{\Phi}^2+2\,\dddot{\Phi}\,t}}{\dddot{\Phi}}+\phi\right]\right\} \end{aligned} \tag{4}$$

where $\phi = \pm\ddot{\Phi}\tau/\,\dddot{\Phi}$ is a phase constant, $r(t)$ is the pulse envelope. If the input short pulse from the MLFL is Gaussian shaped, the output pulse envelope $r(t)$ can be analytically expressed using the Airy function [8], [9].

The instantaneous RF carrier frequency of the obtained waveform can be written as

$$\omega_{RF}(t) = \frac{d\Psi(t)}{dt} = \tau(\ddot{\Phi}^2 + 2\,\dddot{\Phi}\,t)^{-1/2}. \tag{5}$$

It is shown that the waveform is nonlinearly chirped. The central frequency at $t = 0$ can be expressed as $\omega_c = |\tau/\ddot{\Phi}|$, which means that the central frequency of the generated chirped pulse is only dependent upon the first-order dispersion for an SF with a given free spectral range (FSR). The ratio $\dddot{\Phi}\ \tau/|\ddot{\Phi}|^3$ determines the chirp rate of the generated pulse, which can be found more directly from the first-order approximation of (5)

$$\omega_{RF}(t) \cong \tau/|\ddot{\Phi}| - \left(\dddot{\Phi}\ \tau/|\ddot{\Phi}|^3\right)t. \tag{6}$$

In a radar system, pulse compression is usually realized through matched filtering at the radar receiver. The matched filtering is implemented by correlating a template, which is a chirped RF pulse in the pulse compression radar, with a received signal to detect the presence of the template. It is known that a matched filter provides the optimal signal-to-noise ratio (SNR) when the received template is imbedded in an additive white noise [1], [10]. The pulse compression ratio is determined by the time-bandwidth product of the transmitted RF pulse. In other words, a larger chirp rate of the RF pulse would lead to a higher pulse compression ratio. Mathematically, the operation of matched filtering is equivalent to an autocorrelation. For a real-valued signal $i(t)$, its autocorrelation function $R(t)$ is defined as

$$R(t) = i(-t) * i(t) = \int_{-\infty}^{\infty} i(t+\tau)i(\tau)d\tau \tag{7}$$

where $*$ denotes the convolution operation.

It should be noted that a linear frequency modulation may not be always necessary in a pulse compression radar. The fre-

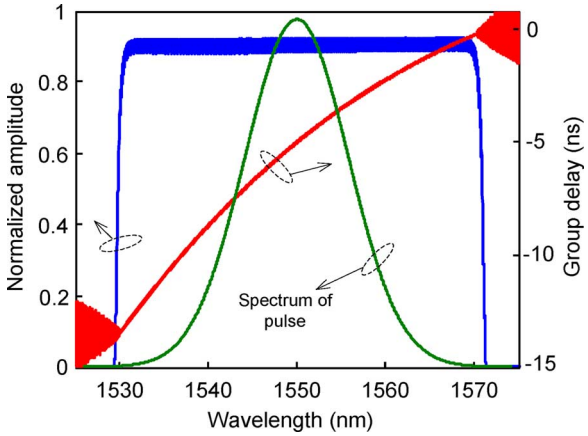

Fig. 2. Reflectivity and group delay of the designed apodized NLCFBG. The spectrum of the input ultra-short short pulse is also shown.

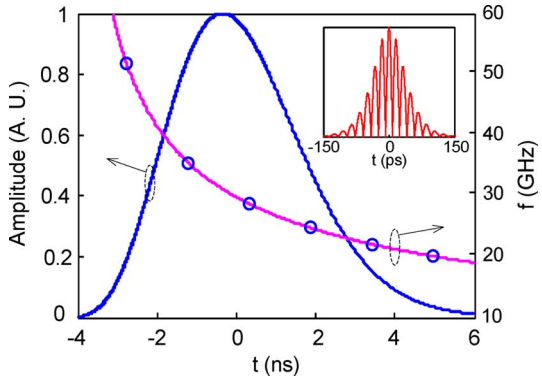

Fig. 3. Envelope and the instantaneous frequency of the generated RF pulse ($\ddot{\Phi} = 500$ ps^2, $\dddot{\Phi} = 30$ ps^3, $\omega_c/2\pi = 30$ GHz) in the first simulation. In the results of instantaneous frequency, the curve is the predicted data by (2) and the circles are the simulation results. Inset: the compressed pulse obtained by autocorrelation.

quency modulation can be of almost any forms, provided that the pulse compression filter is designed to match the transmitted waveform. In our approach, the required central frequency and the chirp rate can be obtained by using an NLCFBG with the required first- and second-order dispersions and an SF with a predetermined τ. The NLCFBG can be fabricated by bending a linearly chirped fiber Bragg grating (LCFBG) with a nonlinearly distributed external strain. To fabricate an NLCFBG with a larger nonlinear dispersion, a nonlinearly chirped phase mask may be used.

III. Results and Discussions

Numerical simulations are implemented to demonstrate the feasibility of the proposed scheme. In the numerical simulations, the optical pulse from the MLFL is a transform-limited Gaussian pulse with a full-width at half maximum (FWHM) of 350 fs and a central wavelength of 1550 nm. The central frequency of the generated waveform is set to be 30 GHz by using an SF with a time delay difference of $\tau = 94.2$ ps. In the first simulation, the dispersion coefficients $\ddot{\Phi}$ and $\dddot{\Phi}$ are chosen to be 500 ps^2 and 30 ps^3, respectively. The NLCFBG has a grating period variation from 527.59 to 541.38 nm. The reflectivity and the group delay of the NLCFBG, calculated by using the piecewise-uniform approach [11], are shown in Fig. 2. For comparison, the spectrum of the input short pulse from the MLFL is also shown in Fig. 2. To provide a large dispersion with a bandwidth covering the entire pulse spectrum, the grating should have a length of about 1.5 m.

The generated RF pulse and its instantaneous frequency are shown in Fig. 3. The predicted instantaneous frequency values according to (2) agree well with the simulation results. The inset in Fig. 3 shows the compressed waveform obtained through matched filtering or autocorrelation calculated based on (7), which demonstrates a pulse compression ratio of 63. Note that the pulse compression ratio is estimated by comparing the FWHM of the chirped pulse and that of the autocorrelation waveform.

For an NLCFBG with a larger second-order dispersion, high and fast-oscillating ripples at one side of the generated waveform would be observed, as shown in Fig. 4(a), where $\dddot{\Phi}$ is

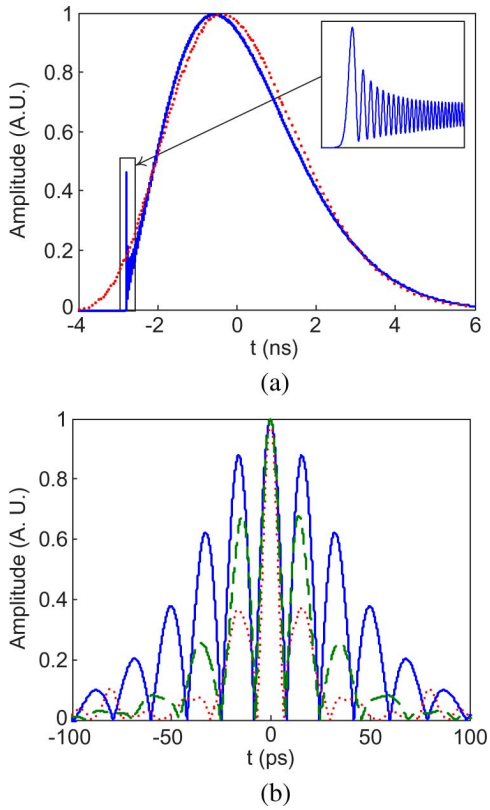

Fig. 4. (a) Envelopes of the generated RF pulses, $\ddot{\Phi} = 500$ ps^2, $\omega_c/2\pi = 30$ GHz, solid: $\dddot{\Phi} = 45$ ps^3, dotted: $\dddot{\Phi} = 30$ ps^3. (b) Compressed waveforms by autocorrelation, solid: $\dddot{\Phi} = 30$ ps^3, dashed: $\dddot{\Phi} = 45$ ps^3, dotted: $\dddot{\Phi} = 60$ ps^3.

set to be 45 ps^3 while keeping $\ddot{\Phi}$ as 500 ps^2 and τ as 94.2 ps. A zoom-in display of the ripples is shown in the inset of Fig. 4(a). For comparison, the pulse envelope for $\dddot{\Phi} = 30$ ps^3 is also displayed (dotted curve). These ripples will degrade the pulse compression performance. However, it is found that the major spectral components of these ripples are higher than 100 GHz, which can be removed by using a low-pass filter. Fig. 4(b) shows the autocorrelation waveforms obtained with $\dddot{\Phi}$ as 30, 45, and 60ps^3, with a low-pass filter applied to remove the oscillating ripples. It is shown that a higher $\dddot{\Phi}$ leads to a better

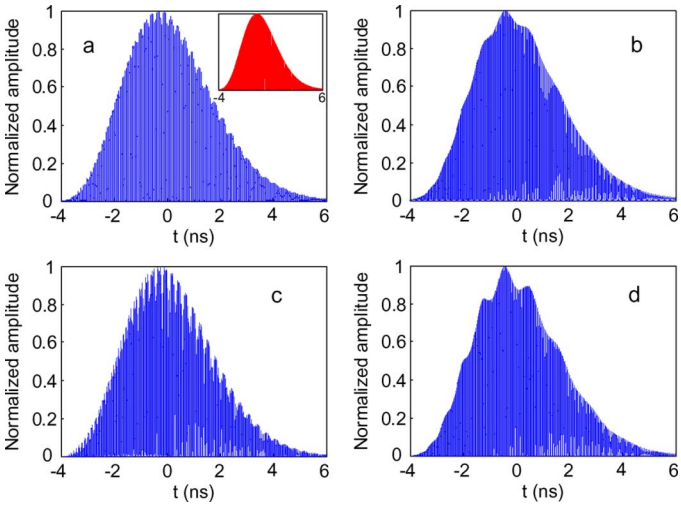

Fig. 5. Generated waveforms with different GDRs. (a) GDR amplitude is 40 ps and period is 30 GHz. (b) Amplitude is 40 ps and period is 60 GHz. (c) Amplitude is 80 ps and period is 30 GHz. (d) Amplitude is 80 ps and period is 60 GHz.

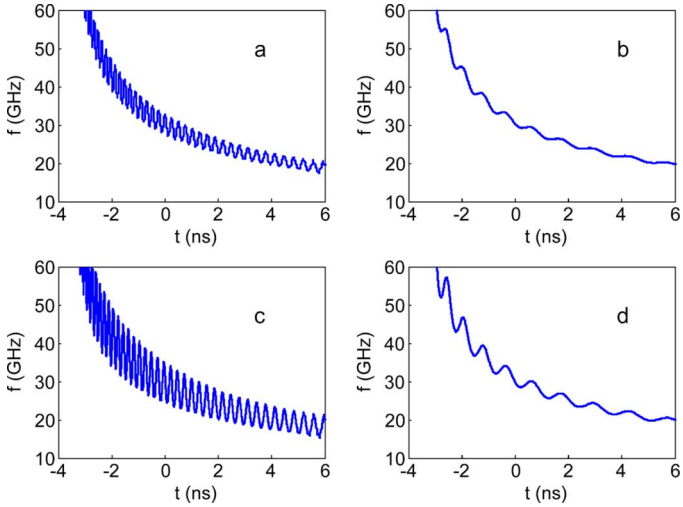

Fig. 6. Instantaneous frequency of the generated waveforms with GDRs. (a) GDR amplitude is 40 ps and period is 30 GHz. (b) GDR amplitude is 40 ps and period is 60 GHz. (c) GDR amplitude is 80 ps and period is 30 GHz. (d) GDR amplitude is 80 ps and period is 60 GHz.

suppression of the sidelobes in the autocorrelation waveforms, which is important to improve the range resolution in a radar system. The pulse compression ratios for the three cases with $\dddot{\Phi}$= 30 ps^3, $\dddot{\Phi}$= 45 ps^3, $\dddot{\Phi}$= 60 ps^3 are estimated to be 63, 115, and 450, respectively.

In theory, a smooth group delay response of an NLCFBG can be achieved by applying apodization during the fabrication process. However, an apodized NLCFBG usually exhibits pseudoperiodic GDRs due to the errors in grating period and the refractive index modulation arising from imperfections in the fabrication process [12], [13]. To evaluate the GDRs on the performance of a chirp RF pulse generation system, one can use the measured GDR data of a specific grating, which is accurate and simple, but is limited to the specific grating with the specific GDRs. To have a general understanding of the GDRs on the performance of a chirp RF pulse generation system, in this paper we would model the GDRs to have a sinusoidal distribution with different amplitudes and periods. The modeling of GDRs using a sinusoidal function has been widely used in analyzing the GDR performance in optical communications systems [14], [15].

To investigate the influence of the GDR on the generated waveform in a nonlinear wavelength-to-time mapping system, we use an NLCFBG with an ideal group delay that is superimposed with a sinusoidal GDR. We choose the same parameters as those in the first numerical example, i.e., $\ddot{\Phi} = 500$ ps^2, $\dddot{\Phi}$= 30 ps^3, $\omega_c/2\pi = 30$ GHz. Two sets of GDR data are considered: the peak-to-peak amplitudes of the sinusoidal group delay ripples are 40 and 80 ps and the periods of the sinusoidal ripples are 30 and 60 GHz. The generated waveforms with different GDRs are shown in Fig. 5, where the inset in Fig. 5(a) shows a generated waveform in a system without GDRs. It is shown that envelope ripples are observed in the generated waveforms due to the existence of the GDRs. It is also found that a larger ripple amplitude in the group delay would lead to a greater ripple amplitude in the waveform envelope; and a smaller ripple period in the group delay would lead to a smaller ripple period

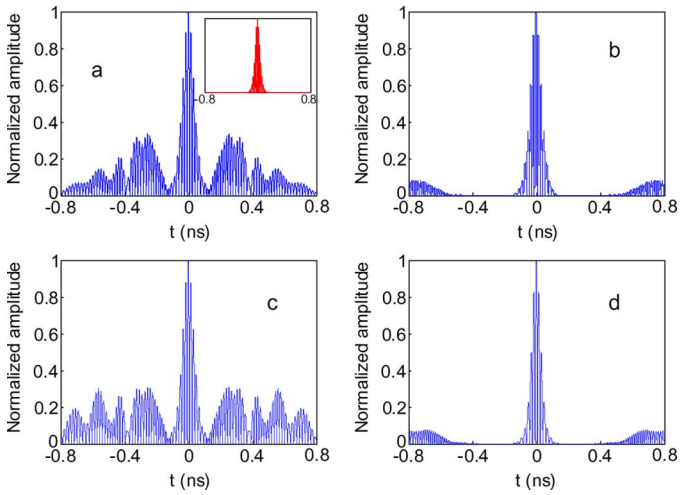

Fig. 7. Autocorrelation waveforms with different GDRs. (a) GDR amplitude is 40 ps and period is 30 GHz. (b) GDR amplitude is 40 ps and period is 60 GHz. (c) GDR amplitude is 80 ps and period is 30 GHz. (d) GDR amplitude is 80 ps and 60 period is GHz.

in the waveform envelope. The observation can be intuitively explained by the principle of wavelength-to-time mapping. The instantaneous frequency of the generated waveforms is plotted in Fig. 6. It is found that the ripples are also included in the instantaneous frequency curve as compared to the case without GDRs, as shown in Fig. 3. Again, the amplitude and the period of the ripples in the instantaneous frequency curve are positively correlated to those of the ripples in the group delay. Fig. 7 shows the autocorrelation results. Compared with the autocorrelation results without GDR, as shown in the inset of Fig. 7(a), sidelobes are observed in the autocorrelation waveforms due to the existence of the GDRs. However, the FWHM of the autocorrelation waveforms are almost kept unchanged. Therefore, we can conclude that the system proposed to generate chirped RF pulses based on nonlinear wavelength-to-time mapping using an NLCFBG is robust to the GDRs.

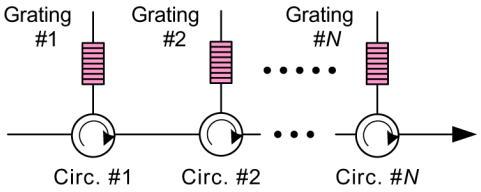

Fig. 8. Cascading of a number of short NLCFBGs to produce an equivalent long NLCFBG with large dispersion parameter. (Circ: optical circulator).

The key device in the proposed chirped RF pulse generation system is the NLCFBG, which is nonlinearly chirped with a long length. A few techniques have been proposed to fabricate chirped FBGs with nonlinear chirping. One simple way is to use a customer-designed nonlinearly chirped phase mask, but at a higher cost with less flexibility. A flexible and cost-effective technique to fabricate an NLCFBG is to use asymmetrical stretching, which can be implemented using a regular LCFBG. A nonlinear chirping is introduced by applying a nonlinearly distributed force, realized by asymmetrically stretching the LCFBG. Based on this technique [16], an NLCFBG with a dispersion coefficient varying from -300 nm/ps (~ 385 ps^2) to -1000 nm/ps (1280 ps^2) in a 0.75-nm range was achieved. The fabricated NLCFBG has a second-order dispersion coefficient $\ddot{\Phi}$ of 20 ps^2.

The NLCFBG used in our proposed system should have a length longer than 1 m due to the requirement for a large bandwidth to cover the entire spectrum of the FSPL and a large dispersion coefficient to generate high chirp RF pulses. Several techniques have been demonstrated for the fabrication of long gratings [17]–[19]. A technique to fabricate a 57-cm-long chirped grating with an arbitrary profile was demonstrated in [17]. In [18], the fabrication of a high-quality long FBG (up to 1 m) with a subnanometer precision was also demonstrated. In [19], the fabrication of long chirped FBG using an intensity-modulated laser beam based on the holographic technique was proposed, and a chirped FBG with a length as long as 3 m was fabricated. Since no phase mask is required, the fabrication is very flexible. The key difficulty involved in the use of the holographic technique is the extremely high sensitivity to environmental changes, which makes the system extremely hard to control. An alternative solution to produce an NLCFBG with a large dispersion coefficient and wide bandwidth is to use multiple cascaded NLCFBGs, each having a short length and a lower dispersion. For example, the dispersion coefficient and wide bandwidth of a 1.5-m-long NLCFBG can be equivalently obtained by cascading five short NLCFBGs, each having a length of 30 cm. The key advantage of this technique is that the multiple gratings can be readily fabricated with current, mature technology. As shown in Fig. 8, a number of short NLCFBGs with smaller but identical dispersion coefficient are cascaded to generate an equivalent NLCFBG with a larger dispersion coefficient. Due to the use of optical circulators, the total loss of the equivalent NLCFBG is higher than the use of a single long NLCFBG.

IV. Conclusion

Chirped RF pulse generation based on optical spectral shaping and nonlinear wavelength-to-time mapping in an NLCFBG was investigated. In the proposed approach, the optical pulse from the MLFL was spectrum-shaped by an SF with a sinusoidal frequency response; the spectrum-shaped pulses were then sent to the NLCFBG to perform nonlinear wavelength-to-time mapping. Thanks to the nonlinear dispersion in the NLCFBG, RF pulses with frequency chirping were generated. The central frequency and the chirp rate of the generated RF pulses were determined respectively by the first- and second-order dispersions of the NLCFBG. The feasibility of the approach was verified by numerical simulations. Chirped pulse generation with a pulse compression ratio as high as 450 was demonstrated.

In an NLCFBG, a smooth group delay response can be achieved by applying apodization during the fabrication process. However, an apodized NLCFBG usually exhibits pseudoperiodic GDRs due to the errors in grating period and the refractive index modulation arising from imperfections in the fabrication process. In this paper, the performance of the chirp pulse generation system due to the GDRs was investigated in detail. We found that the system performance degradation due to the GDRs in the NLCFBG was small, which can be kept within safe bounds. The approach offers a potential solution for chirped RF pulse generation with high central frequency and large chirp rate for applications in pulse compression radar systems.

References

[1] M. I. Skolnik, *Introduction to Radar*. New York: McGraw-Hill, 1962.
[2] A. Zeitouny, S. Stepanov, O. Levinson, and M. Horowitz, "Optical generation of linearly chirped microwave pulses using fiber Bragg gratings," *IEEE Photon. Technol. Lett.*, vol. 17, no. 3, pp. 660–662, Mar. 2005.
[3] H. Chi and J. P. Yao, "An approach to photonic generation of high-frequency phase-coded RF pulses," *IEEE Photon. Technol. Lett.*, vol. 19, no. 10, pp. 768–770, May 2007.
[4] H. Chi and J. P. Yao, "All-fiber chirped microwave pulses generation based on spectral shaping and wavelength-to-time conversion," *IEEE Trans. Microw. Theory Tech.*, vol. 55, no. 9, pp. 1958–1963, Sep. 2007.
[5] X. Fang and R. O. Claus, "Polarization-independent all-fiber wavelength-division multiplexer based on a Sagnac interferometer," *Opt. Lett.*, vol. 20, no. 20, pp. 2146–2148, Oct. 1995.
[6] M. A. Muriel, J. Azana, and A. Carballar, "Real-time Fourier transformer based on fiber gratings," *Opt. Lett.*, vol. 24, no. 1, pp. 1–3, Jan. 1999.
[7] H. Chi, F. Zeng, and J. P. Yao, "Photonic generation of microwave signals based on pulse shaping," *IEEE Photon. Technol. Lett.*, vol. 19, no. 9, pp. 668–670, May 2007.
[8] M. Miyagi and S. Nishida, "Pulse spreading in a single-mode fiber due to third-order dispersion," *Appl. Opt.*, vol. 18, no. 5, pp. 678–682, Mar. 1979.
[9] M. Amemiya, "Pulse broadening due to higher order dispersion and its transmission limit," *J. Lightw. Technol.*, vol. 20, no. 4, pp. 591–597, Apr. 2002.
[10] M. A. Richards, *Fundamentals of Radar Signal Processing*. New York: McGraw-Hill, 2005.
[11] T. Erdogan, "Fiber grating spectra," *J. Lightw. Technol.*, vol. 15, no. 8, pp. 1277–1294, Aug. 1997.
[12] R. L. Lachance, M. Morin, and Y. Painchaud, "Group delay ripple in fibre Bragg grating tunable dispersion," *Electron. Lett.*, vol. 38, no. 24, pp. 1505–1507, Nov. 2002.
[13] R. Kashyap and M. de L. Rocha, "On the group delay characteristics of chirped fibre Bragg gratings," *Opt. Commun.*, vol. 153, no. 1, pp. 19–22, Jul. 1998.
[14] K. Ennser, M. Ibsen, M. Durkin, M. N. Zervas, and R. I. Laming, "Influence of nonideal chirped fiber grating characteristics on dispersion cancellation," *IEEE Photon. Technol. Lett.*, vol. 10, no. 10, pp. 1476–1478, Nov. 1998.

[15] J. C. Cartledge, "Effect of modulator chirp and sinusoidal group delay ripple on the performance of dispersion compensating gratings," *J. Lightw. Technol.*, vol. 20, no. 11, pp. 1918–1923, Nov. 2002.
[16] A. E. Willner, K.-M. Feng, J. Cai, S. Lee, J. Peng, and H. Sun, "Tunable compensation of channel degrading effects using nonlinearly chirped passive fiber Bragg gratings," *IEEE J. Sel. Topics Quant. Electron.*, vol. 5, no. 5, pp. 1298–1311, Sep./Oct. 1999.
[17] M. Ibsen, M. K. Durkin, M. N. Zervas, A. B. Grudinin, and R. I. Laming, "Custom design of long chirped Bragg gratings: Application to gain-flattening filter with incorporated dispersion compensation," *IEEE Photon. Technol. Lett.*, vol. 12, no. 5, pp. 498–500, May 2000.
[18] M. Ibsen, M. K. Durkin, M. J. Cole, M. N. Zervas, and R. I. Laming, "Recent advances in long dispersion compensation fibre Bragg gratings," in *IEE Colloquium on Optical Fibre Gratings*, Birmingham, U.K., Mar. 26, 1999, pp. 6/1–6/7.
[19] J. F. Brennan, III, M. R. Matthews, W. V. Dower, D. J. Treadwell, W. Wang, J. Porque, and X. Fan, "Dispersion correction with a robust fiber grating over the full C-band at 10-Gb/s rates with $<$0.3-dB power penalties," *IEEE Photon. Technol. Lett.*, vol. 15, no. 12, pp. 1722–1724, Dec. 2003.

Hao Chi received the Ph.D. degree in electronic engineering from Zhejiang University, Hangzhou, China, in 2001.

He joined the Department of Information and Electronic Engineering, Zhejiang University, in 2003. Before that, he spent half a year in the Hong Kong Polytechnic University as a Research Assistant and two years in Shanghai Jiaotong University as a Postdoctoral Fellow. Since July 2006, he has been with the Microwave Photonics Research Laboratory, School of Information Technology and Engineering, University of Ottawa, ON, Canada, as a Visiting Scholar. His research interests include optical communications and networking, microwave photonics, fiber-optic sensors, optical signal processing, and fiber grating-based components.

Jianping Yao (M'99–SM'01) received the Ph.D. degree in electrical engineering in 1997 from the Université de Toulon, Toulon, France.

He joined the School of Information Technology and Engineering, University of Ottawa, ON, Canada, in 2001, where he is a Professor, Director of the Microwave Photonics Research Laboratory, and Director of the Ottawa-Carleton Institute for Electrical and Computer Engineering. From 1999 to 2001, he held a faculty position with the School of Electrical and Electronic Engineering, Nanyang Technological University, Singapore. He holds a guest professorship of Shantou University and Sichuan University, China. He spent three months as an Invited Professor in the Institut National Polytechnique de Grenoble, France, in 2005. His research has focused on microwave photonics, which includes all-optical microwave signal processing, photonic generation of microwave, millimeter-wave, and THz, radio-over-fiber, UWB over fiber, fiber Bragg gratings for microwave photonics applications, and optically controlled phased array antenna. His research interests also include fiber lasers, fiber-optic sensors, and bio-photonics. He has published over 80 papers in refereed journals and over 90 papers in conference proceeding. He is an Associate Editor of the *International Journal of Microwave and Optical Technology*.

Dr. Yao is a member of the Editorial Board of IEEE TRANSACTIONS ON MICROWAVE THEORY AND TECHNIQUES. He received the 2005 International Creative Research Award of the University of Ottawa. He was the recipient of the 2007 George S. Glinski Award for Excellence in Research. He was named University Research Chair in Microwave Photonics in 2007. He is a Registered Professional Engineer of Ontario. He is a member of SPIE, OSA, and a member of the IEEE/LEOS and IEEE/MTT societies.